

# Methodology: Permian Methane Analysis Project (PermianMAP)

## Data Collection and Analysis

Last Update: Oct. 12, 2020

### Aerial Surveys: Scientific Aviation

Scientific Aviation quantifies methane emissions at various spatial scales from a cluster of a few well pads to the entire study area using the aerial mass balance approach<sup>1</sup>. In brief, a single-engine Mooney aircraft is outfitted with a Picarro CRDS instrument (G2210-m) to measure in-situ atmospheric CH<sub>4</sub>, CO<sub>2</sub>, H<sub>2</sub>O mole fractions, a differential GPS and aircraft data computer to enable computation of horizontal wind speeds and directions, and a Vaisala probe to measure ambient temperature and relative humidity. These in-flight measurements are synthesized to estimate a snapshot of methane emissions from the areas circumscribed by the plane. Based on earlier controlled release experiments, the detection limit of the mass balance approach can be as low as 5–10 kg CH<sub>4</sub>/hr; however the exact detection limit is highly dependent on dynamic parameters such as upwind methane concentration and local meteorology (see section ‘Uncertainty, Detection Limits, and Scale’ below for more details)

For PermianMAP, Scientific Aviation is being deployed for four types of measurements: regional mass balances (described in greater detail in the section ‘Aircraft Based Regional Emissions Quantification’) box mass balances, site cluster mass balances, and flare combustion efficiency. Box mass balances occur systematically around 25 pre-defined 20x20 km boxes within our 100 x 100 km Delaware basin study area. Most aerial measurements are site cluster measurements that the aircraft measures with 1–2 km radius spiral flights to measure the emission plume(s) from near ground level to their vertical extent. These areas are selected using two strategies based on the observations from 20x20 km boxes: randomly selected locations and randomly selected single-operator clusters. For each 20x20 km box, five to ten 2x2 km sub-grids are randomly selected for 1 – 2 km circular mass balances centered on the sub-grids; these areas often contain wells from multiple operators. For the second approach, we pre-define irregular shapes in each 20x20 km based on a geospatial analysis that clustered wells into single operator groups. For each 20x20 box, several of these single operator areas are randomly selected for mass balance measurements. For measurements to quantify flare combustion efficiency, the aircraft flies directly through flare plumes to measure concentrations of methane and carbon dioxide; the ratio of these species will be used to estimate the percentage of methane combusted by the flare.

PermianMAP publishes Scientific Aviation data for site cluster mass balances that have passed quality assurance. New data will be added from both additional flights and quality assurance of existing data. While a best effort has been made to provide accurate emission estimates, all data should be considered preliminary and subject to change.

## Attributing Wells to Emission Events

We determine which wells are associated with a given emission event using several well characteristics. The well must have been actively in operation or actively producing during our study period (October 2019 – present) and must have a first production date prior to the given emission event. This allows us to maintain up-to-date well data while avoiding associating new wells with older emission events. Well datasets of actively producing wells are updated on a monthly cadence based on the data reported by operators to Texas<sup>2</sup> and New Mexico<sup>3</sup> state agencies. Attributed wells are a potential source of a given emission event; however, it is possible that midstream facilities or pipelines are responsible. Tank battery locations displayed on PermianMAP are based on satellite imagery analysis by Descartes Labs<sup>4</sup> and locations of Gas Processing Plants are provided by the EPA Greenhouse Gas Reporting Program<sup>5</sup>. Plans to incorporate additional midstream facilities are underway and will be released at a later date.

## Ground Surveys: University of Wyoming

The University of Wyoming (UW) team quantifies site-level methane and VOC emissions using two vehicle-based approaches: Other Test Method 33A (OTM) and the transect method. OTM is an inverse Gaussian dispersion method developed by the US EPA<sup>6</sup>. In summary, a vehicle equipped with a pollutant sensor and 3D sonic anemometer is deployed 40–200 meters downwind of an emission source for approximately 20 minutes at a stationary location near the plume centerline. Site-level emission rates are estimated by fitting concentration and wind data to a Gaussian curve<sup>7, 8</sup>. The transect method uses the same vehicle-based measurement platform, but samples the plume as the vehicle drives back and forth on a downwind road in a direction transverse to wind<sup>9</sup>. The precision of OTM and transect methods (for 10+ passes) have been estimated to be +233%/-41% and +170%/-50%, respectively<sup>9, 10</sup>.

In January 2020, UW deployed their mobile air quality laboratory to the study area to perform OTM and transect measurements at randomly selected well pads and tank batteries. Methane and speciated VOCs were measured continuously with a Picarro CRDS and PTR-TOF-MS<sup>9, 10</sup>. Site selection followed a pseudo-random process that accounted for the methodological constraint of downwind public road access. We randomly selected several 20x20 km areas within our gridded 100x100 km access, excluding any area with limited public roads. The UW team randomly selected sites within each 20x20 km area for OTM and/or transect measurements that were downwind of the current wind direction. In addition to quantifying emissions, the UW team used a FLIR camera to inspect the site for emissions from the fence line. At some sites, a canister air sample was collected for VOC analysis to supplement PTR-TOF-MS data<sup>11</sup>. For sites where it was confirmed that the mobile laboratory was downwind of the site, but no enhanced methane was detected for at least 10 minutes, emissions were reported as below detection limit, which has been estimated as 0.036 kg CH<sub>4</sub>/hr for the OTM method<sup>7</sup>.

## Flaring Survey

EDF compiled a list of potential locations of recently active flares in the Permian region (Delaware and Midland Basins) based on a geospatial analysis of the SkyTruth Global Flaring Dataset<sup>12</sup>. The SkyTruth data includes probable locations of oil and gas flares detected as heat sources by the Visible Infrared Imaging Radiometer Suite (VIIRS) instrument on the NOAA Suomi NPP satellite. To account for spatial uncertainty of SkyTruth flare locations, we spatially joined their individual flare detections from 10/1/2019 to 1/31/2020 using a 100-meter buffer distance; the centroid latitude/longitude of the 1,014 joined detections were defined as likely locations of recently active O&G flares.

Leak Surveys Incorporated (LSI)<sup>13</sup>, a leak detection company specializing in aerial optical gas imaging, was provided a list of 573 potential active flare locations from the original set of 1,014. Site selection balanced representativeness and efficiency by defining one contiguous, high flare density area in each basin that could be surveyed in a total of approximately five days. For the Delaware, we selected 323 locations corresponding to part of the main PermianMAP study area defined by the NW and SE corners 32.325° N, 103.822° W and 31.417° N, 103.202° W, plus three additional flares on University Lands located within 6 km

of the study area. For the Midland, we selected 250 locations from the two counties with the highest flare counts: Midland and Martin.

LSI surveyed these locations with a custom infrared camera (IR) deployed in a R44 helicopter. Flare locations were identified with a latitude/longitude and unique flare ID. During the week of February 17, 2020 (Survey 1), LSI surveyed the selected 573 potential flare locations to determine the presence of a flare; if a flare was identified near the spatial coordinates, LSI recorded 15 – 30 seconds of both visual spectrum and IR video of the flare and nearby equipment. For flares with apparent combustion issues, LSI recorded an additional 30 – 60 seconds of footage of the flare plume from multiple angles to provide visual evidence of flare status. For each flare, LSI assigned a qualitative assessment of the apparent flare status at the time of survey from four categories: inactive and unlit with no emissions (inactive); active, lit, and operating properly (operational); active and lit but with operational issues such as incomplete combustion or excessive smoke (malfunction); or active, unlit, and venting methane (unlit and venting). If multiple flares were present at approximately the same distance from the reported coordinates, then the LSI randomly select a flare to assign to the Flare ID. If no active or inactive flares are visible from the reported coordinates, then the team reported no flare was present at the location.

During the week of March 23, 2020 (Survey 2), LSI was deployed for a follow-up survey at 337 flare locations: all of the malfunctioning or unlit flares from Survey 1 plus a random selection of half the operational or inactive flares from the first survey. LSI used a similar protocol as the first survey, but only recorded video for flares with a malfunctioning or unlit status. Additionally, LSI was deployed to systematically survey all O&G flares in a 20 x 20 km box defined by the NW and SE corners 31.780° N, 103.406° W and 31.596° N, 103.199° W. A third flaring survey occurred from Jun 22 – July 1, 2020 with a similar methodology to the second survey for repeated observations of problematic flares and random sampling of the identified flares. The systematic survey was also repeated during Survey 3.

The systematic survey results, which are not included in the current analysis, will be used in later analyses to assess if the flares based on the VIIRS dataset are representative of the full population; it is likely the satellite-detected flares are larger on average and therefore may have different performance than smaller flares.

For Survey 1, LSI found 337 flares at the provided locations, 312 of which were active during the survey. About 11% of flares had issues that could cause abnormally high methane emissions: 7% were lit but with combustion issues, while 4% were unlit and venting. For Survey 2, the analysis accounts for the sampling strategy bias towards malfunctioning/unlit flares by adding predicted results from the 50% of operational/inactive flares that were not re-surveyed. After this adjustment, the second survey results are similar to the first survey: about 12% of flares had issues (7% combustion issues, 5% unlit). Twenty-five percent (9/36) of flares were observed to have issues during both surveys. Including approaches for estimating the performance of unsampled flares, the third survey found similar results with 11% of flares malfunctioning and 4.5% to be unlit and venting – including two flares which were found to be malfunctioning during the course of all three surveys (Flare ID 448 and 630).

To estimate methane emissions from flaring, we used our qualitative flare performance data and reasonable assumptions about the combustion efficiency of operational, malfunctioning, and unlit flares to estimate overall combustion efficiency; and then applied that data to estimated flared volumes in 2019 based on an analysis of VIIRS data<sup>14</sup>. Gas flared volumes were estimated using nighttime fire and flare data observed by VIIRS instrument on board the Suomi National Polar-Orbiting satellite. We filtered the daily VIIRS data from January to December 2019 for observations with flare source temperatures in the range of 1400 to 2500 K, which are representative of gas flares. The gas flaring volumes were estimated using the empirical relationship<sup>15</sup>:

$$V_{\text{annual}}=0.0274RH^{\wedge}$$

Here  $V_{\text{annual}}$  is the gas flared volume in bcm and  $RH^{\wedge}$  is the average adjusted radiant heat of the observed flares, adjusted to account for the observed non-linearity in the relationship between flared gas volumes and

radiant heat parameters. Using this approach, mean flaring volumes in the Permian Basin are estimated at 7.9 bcm (or 280 bcf) in 2019, with 6.5 bcm (230 bcf) in the Texas portion of the Permian and the remainder (1.4 bcm or 49 bcf) in the New Mexico Permian Basin.

We assume that operational flares perform at the EPA default combustion efficiency of 98%<sup>16</sup>, which means 2% of the methane sent to the flare is emitted rather than being combusted to carbon dioxide. Unlit flares have a combustion efficiency of 0% since all the methane is emitted unburnt. For the flares that were lit, but with apparent combustion issues, we assumed 90% combustion efficiency. These assumptions lead to an overall combustion efficiency of 93%, which means 7% of flared methane is emitted (Table 1). Applying 93% combustion efficiency to the 280 bcf of gas flared in the Permian in 2019 (assuming 80% CH<sub>4</sub> content) results in annual methane emissions of approximately 300,000 metric tons from flaring in the Permian; unlit flares account for about 65% of these emissions, while operational and poorly combusting flares account for about 15 and 10%, respectively. Based on the state-specific flared gas volumes, Texas and New Mexico are responsible for about 250,000 and 50,000 metric tons (MT) of CH<sub>4</sub> emissions, respectively. In comparison, applying the EPA default assumption combustion efficiency of 98% results in about 80,000 – 90,000 MT CH<sub>4</sub> emissions. Our emissions estimate is about 3.5 times higher than alternative estimates based on EPA assumptions of combustion efficiency. EPA publishes two separate estimates of Permian flaring methane emissions, which incorporates the 98% combustion efficiency but different gas flared data. The 2020 EPA Greenhouse Gas Inventory<sup>17</sup> reports 2018 Permian Basin methane emissions of 12,100 MT CH<sub>4</sub> from associated gas flaring, plus 8,500 MT and 4,600 MT from associated gas venting and miscellaneous production flaring, respectively. For comparison, the EPA Greenhouse Gas Reporting Program<sup>5</sup> reports 18,800 MT CH<sub>4</sub> from Permian Basin onshore production facilities.

| Total                     | Survey 1 | Survey 2 | Survey 3 | Average |
|---------------------------|----------|----------|----------|---------|
| Operational               | 276      | 147      | 237      |         |
| Inactive                  | 25       | 0        | 62       |         |
| Combustion Issue          | 23       | 9        | 18       |         |
| Unlit and Venting         | 13       | 10       | 12       |         |
| Not surveyed              | 94       | 265      | 102      |         |
| Active Flares             | 312      | 166      | 267      |         |
| Malfunctioning (CI + U&V) | 36       | 19       | 30       |         |
|                           |          |          |          |         |
| % Malfunctioning          | 11.5%    | 11.4%    | 11.2%    | 11.4%   |
| % Unlit and Venting       | 4.2%     | 6.0%     | 4.5%     | 4.9%    |

## Regional Emissions Estimates

**Atmospheric [CH<sub>4</sub>] Transport Modeling:** An atmospheric reanalysis similar to previous studies<sup>18, 19</sup> was used to create simulated regional atmospheric [CH<sub>4</sub>] estimates simulating only atmospheric [CH<sub>4</sub>] from emissions within the 100 x 100km Delaware basin study area. Preliminary estimates of surface fluxes of [CH<sub>4</sub>] within the Delaware study area taken from the EPA 2012 gridded inventory<sup>20</sup>, save for the Permian Basin where an updated, production-based inventory is used<sup>21</sup>. The Weather Research and Forecasting – Chemistry model (WRF-CHEM)<sup>22</sup> was used to simulate atmospheric transport of gases in reanalysis system; creating a first estimate of atmospheric [CH<sub>4</sub>] consistent with the regional meteorology and the preliminary estimate of emission sources. This reanalysis is incorporated within both aircraft and tower-based quantification of regional CH<sub>4</sub> emissions from the Delaware study area as described in the sections below.

**Aircraft-Based Regional Emissions Quantification:** As mentioned briefly above under Aerial Surveys, monthly regional mass balance flights operated by Scientific Aviation were conducted to constrain CH<sub>4</sub> emissions from a high production segment of the Delaware basin, referred to as the Delaware study area. On each flight day, two laps consisting of a box enclosing the 100 km x 100 km Delaware basin study area were flown at 1100 ±100 ft above ground level (agl), with one complete lap taking ~ 2 h to complete. Two to three vertical profiles were also flown by the aircraft as pairs of ascents/descents to determine the mixing height of surface emissions. Meteorological conditions, [CH<sub>4</sub>] measured along the flight path and the mixing height determined from the airborne vertical profiles are synthesized in the mass balance method to calculate CH<sub>4</sub> emissions from the area encircled by the flight path. The large area of the flight path (10,000 km<sup>2</sup>) combined with atmospheric variability leads to large uncertainties in the emissions quantified utilizing only the direct measurements from the mass balance approach; however, these uncertainties are addressed by incorporating the transport modeling discussed above within the emissions estimate.

[CH<sub>4</sub>] emissions are computed from each complete circuit by comparing the observed and simulated [CH<sub>4</sub>] enhancement, the increase in [CH<sub>4</sub>] downwind of the study area relative to a background value, and adjusting emissions within the study area to minimize the absolute error between the simulated and observed [CH<sub>4</sub>]. The 10th percentile of [CH<sub>4</sub>] observations in the circuit determines the background and is subtracted from the observed [CH<sub>4</sub>] observations, resulting in an estimate of [CH<sub>4</sub>] enhancements. These observed enhancements are then compared to simulated [CH<sub>4</sub>] enhancements by matching observation and model at the nearest grid points in space and time. Simulated enhancements are split into two categories: Delaware study area enhancements and enhancements originating from outside the Delaware study area. Enhancements associated with sources outside the Delaware study area are subtracted from the observed [CH<sub>4</sub>] enhancements, resulting in a set of observations whose enhancements can be directly attributed to emissions within the Delaware study area. The simulated Delaware study area enhancements are then compared to the observed enhancements, and a scalar multiplier is applied to the simulated enhancements to minimize the absolute error between the two datasets. Because the emissions scale linearly with the simulated enhancements, this scalar multiplier, applied to the preliminary emissions estimate within the study area, provides a solution to the emissions within the Delaware study area. The solution for each of the two circuits are merged into a single daily estimate.

To test the uncertainty of the emission rate solution for each flight day, a 1000-iteration Monte Carlo uncertainty assessment was performed, adjusting various parameters to test how they impacted the solution. This includes the uncertainty in the background, uncertainty in the assumed influence from sources outside the domain, and uncertainty in the atmospheric transport. From the 1000 iterations, the 2.5th and 97.5th percentile of solutions are chosen to represent the 95% confidence interval.

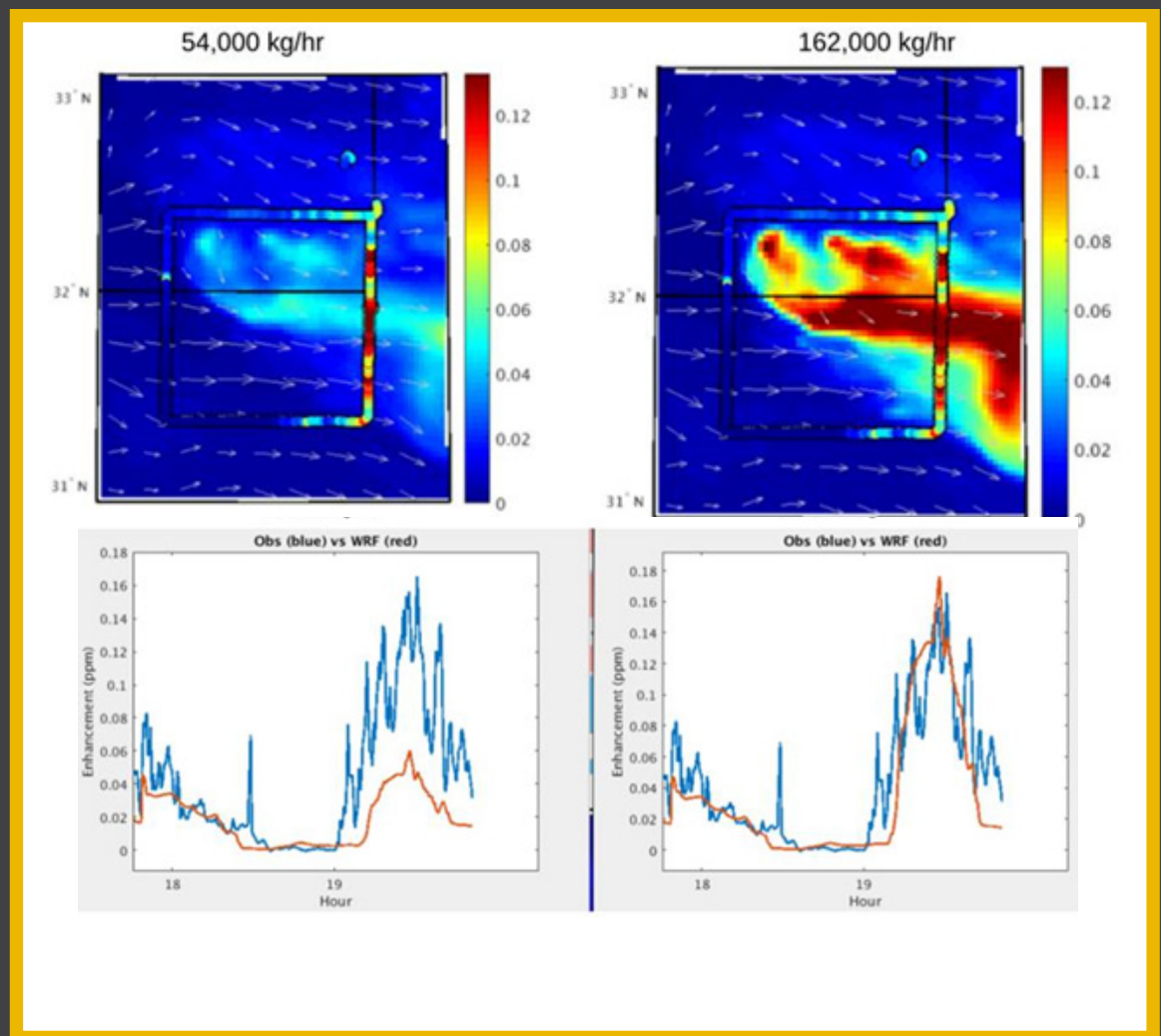
**March 9, 2020 Study-Area Loss Rate:** On March 9, Scientific Aviation utilized the mass balance method to quantify emissions from the Delaware study area. [CH<sub>4</sub>] in parts per billion over background along the flight paths are shown in Figure 1 below. [CH<sub>4</sub>] are substantially higher in the eastern transect, which is due to methane emissions from within the Delaware study area dispersing downwind. Based on the traditional mass balance approach without utilizing the atmospheric chemistry model, emissions from the Delaware study area were estimated to be ~160,000 kg CH<sub>4</sub>/hr. Atmospheric transport modeling optimizes the fit from the prior inventory<sup>21</sup> (54,000 kg CH<sub>4</sub>/hr) upwards by a factor of three to 162,000 kg CH<sub>4</sub>/hr. Figure 1 presents temporal (top) and spatial (bottom) comparisons of the emissions simulated by the prior (left) and posterior (right) conditions. The posterior solution shows marked spatiotemporal agreement with the aircraft observations. The close agreement between the mass balance methodology with and without the transport model supports that methane emissions from the Delaware basin study area on March 9 were approximately 160,000 kg CH<sub>4</sub>/hr. Scientific Aviation also has completed two other mass balance flights of the study region on January 22 and March 25 2020, which had higher uncertainty due to less stable meteorological conditions; however preliminary analyses indicate a similar magnitude of emissions to the March 9 flight. To calculate a loss rate (CH<sub>4</sub> emissions normalized to methane production) in our study area, we use Enverus data to determine all wells in the study area with production during October 2019 – February 2020. As of April 1, 2020, January 2020 was the most recent month with nearly complete production data at the time of this analysis (April 2020). Therefore, we selected January 2020 production as most representative of the March 9 flight. We spatially aggregated January daily average gas production for all wells within the flight



path using data provided by Enverus Drillinginfo<sup>23</sup>. We converted this gas production value of ~7,300,000 mcf/day into a methane production value of 4,672,000 kg CH<sub>4</sub>/hr based on assumptions of 80% methane content and 19.2 kg CH<sub>4</sub>/mcf. **Emissions of 162,000 kg CH<sub>4</sub>/hr is equivalent to about 3.5% of total CH<sub>4</sub> production.**

Our loss rate estimate for the Permian Basin is substantially higher than the national average. The draft EPA 2020 Greenhouse Gas Inventory (GHGI)<sup>24</sup> estimates national O&G supply chain methane emissions are 7.1 Tg, equivalent to approximately a 1.3% loss rate. Our study area contains limited transmission and local distribution, so it is more appropriate to compare to only the production, gathering, and processing segments — which is ~1.1% in the draft 2020 GHGI. **Consequently, our measurement-based estimate is about 3 times higher than the average reported by the EPA inventory.** In comparison, A synthesis study<sup>25</sup> that used site- and basin-level data found national average oil and gas supply chain methane emissions to be 13 Tg/yr, or a 2.3% loss rate; for production, gathering, and processing, the loss rate is ~2.0%. Accordingly, the Permian loss rate is about 75% higher than this current best estimate of national emissions.

**Figure 1.** Prior (left) and posterior (right) modeled and measured methane enhancement (concentration in parts per million over background) for the March 9th flight. The colors in the square perimeter represent measured methane enhancement from Scientific Aviation's flight around the study area. The bottom figures show that the prior inventory of 54,000 kg/hr is inaccurate because modeled and observed enhancement do not match, yet tripling the inventory (162,000 kg/hr) results in a match.



**Tower Based Regional Emissions Quantification:** Continuous measurements of atmospheric [CH<sub>4</sub>] and [CO<sub>2</sub>] were collected at five locations surrounding the Permian Basin Study Area beginning 1 March 2020 using methods similar to a prior study<sup>26</sup>. Note that only four of the five planned measurement sites are used in this analysis for months prior to September 2020 due to intermittent instrument malfunctions at the northernmost site (Maljamar). Of these measurement locations, four were on towers at measurement heights of 80 – 134 m agl and the westernmost site (Carlsbad) was at a mountaintop station on a rooftop 4 m agl. The measurements were made with wavelength-scanned cavity ring down spectroscopic instruments (Picarro, Inc., models G2301, G2401, G2204, and G2132-i). The air samples were dried using Nafion dryers (PermaPure, Inc.) in reflux mode, with an internal water vapor correction applied for the effects of the remaining water vapor (<1%). The instruments were calibrated in the laboratory prior to deployment and using quasi-daily field tanks traceable to the WMO X2004A scale<sup>27, 28</sup>. The [CH<sub>4</sub>] measurement uncertainty (including instrument noise, uncertainty due to water vapor calibration and tank assignment uncertainty) for the tower locations ranged from 0.6-5.4 ppb, with the differences being attributable to different instrument type, short Nafion dryer (Hobbs), and laser aging (Notrees).

[CH<sub>4</sub>] emissions in the study domain were calculated for each day of tower observations using a similar technique as used with the aircraft observations described above. Daily afternoon [CH<sub>4</sub>] at each tower site averaged from 16Z (11 LST) through 22Z (17 LST) was computed from both the observations and the simulation. A background [CH<sub>4</sub>] value (both for the observations and the model) is selected based on the lowest measurement from the available tower sites. This background is subtracted from all tower sites to create an observed CH<sub>4</sub> enhancement, from which simulated enhancements from sources outside of the Delaware study area are subtracted to produce an observed [CH<sub>4</sub>] enhancement associated with sources inside the Delaware study area. A scalar multiplier is then applied to minimize the absolute error between the observed and modeled enhancements, and a daily emission rate is solved for in the Delaware study area.

Unlike the aircraft observations, which are collected on days where meteorological conditions are ideal for measuring emissions from the study domain, the tower dataset is continuous, and many days may not be suitable for calculating an emission rate from the Delaware study area. The most useful tower observations for solving for emissions within the Delaware study area are those whose enhancements are influenced primarily by sources within the Delaware study area and contain minimal enhancements from sources outside of the Delaware study area. We select for these conditions by retaining days when >50% of the simulated downwind afternoon tower enhancements come from sources within the Delaware study area.

The resulting time series of emissions is presented at two temporal scales. First, a ‘weekly moving average’ is calculated numerically as a 7-datapoint moving average of the emissions days that are retained after filtering those with unsatisfactory conditions to constrain emissions within the study area. Additionally a ‘monthly mean’ emission estimate is calculated for all retained days for a given month. New results will be continuously added to the available dataset at a monthly cadence. Results from the tower analyses and remaining mass balance flights for March-June 2020 are presently in review for submission in a peer reviewed manuscript and will be available on Permian Map following publication.

## Uncertainty, Detection Limits, and Scale

As with any emission estimate technique, the approaches used by Scientific Aviation and University of Wyoming have both uncertainty and minimum detection limits. Uncertainty refers to the accuracy (how close to the actual value) and precision (consistency) of measurements. The minimum detection limit (MDL) is the smallest emission rate that an approach can quantify with enough precision to determine if it is statistically significant from zero. The uncertainty and MDL of the mass balance, OTM 33A, and transect approach have been tested with two basic techniques: 1) controlled release tests, and 2) uncertainty propagation. Single blind controlled releases can be used to empirically test the accuracy, precision, and probability of detection at different emission rates and conditions. Uncertainty propagation uses statistical techniques to estimate total uncertainty of an estimate from the uncertainty of input parameters such as wind speed. Based on controlled releases, Scientific Aviation’s mass balance approach for small areas can detect emissions as small as 5–10 kg CH<sub>4</sub>/hr with 10% uncertainty during optimal conditions. However, based on

uncertainty propagation, the Permian project measurements have a median uncertainty closer to  $\pm 60\%$  with few measurements less than 40 kg CH<sub>4</sub>/hr being statistically significant from zero. This higher uncertainty and detection limit are likely due to the high density of methane sources, which increases the variability of upwind methane concentrations. OTM 33A can detect much smaller emissions down to 0.036 kg CH<sub>4</sub>/hr with +233%/-41% uncertainty. Although the OTM 33A has relatively poor precision, controlled tests have shown it has little bias, which means it can be used to accurately characterize a population with a large enough sample size.

On the PermianMAP website ([permianmap.org](http://permianmap.org)), we present measured areas using a colored scale with five bins based on absolute emission rates in kg CH<sub>4</sub>/hr: 1) White: <2 kg CH<sub>4</sub>/hr; 2) Yellow: 2 – 100 kg CH<sub>4</sub>/hr; 3) Orange: 100 – 1000 kg CH<sub>4</sub>/hr; 4) Red: >1000 kg/hr; and 5) Grey: Uncertain. For context, previous studies<sup>25, 29</sup> estimate that the average U.S. well emits between 1 – 2 kg CH<sub>4</sub>/hr. The gray “uncertain” bin includes aerial survey measurements where it could not be determined that the emissions were above zero within a 1 $\sigma$  uncertainty bound. Due to the complexity of the Permian environment, preliminary data indicate the detection limit for Scientific Aviation’s aerial measurements may be as high as ~40 kg CH<sub>4</sub>/hr under certain conditions. Therefore, it is possible that measurement areas labeled “uncertain” could have relatively high emissions that were unable to be quantified due to issues such as interfering sources and poor meteorological conditions at time of measurement.

## Data Availability

All data collected through the surveys, including estimated emission rates and associated uncertainty, are available from the ‘Download Datasets’ tab available on the main platform site<sup>30</sup>. For questions about the data presented on the platform and in this document please contact [permianmap@edf.org](mailto:permianmap@edf.org).

## References:

- <sup>1</sup> <https://www.scientificaviation.com/methods/>
- <sup>2</sup> Railroad Commission of Texas, Production Data [https://www.rrc.state.tx.us/about-us/resource-center/research/data-sets-available-for-download/#digital\\_map](https://www.rrc.state.tx.us/about-us/resource-center/research/data-sets-available-for-download/#digital_map)
- <sup>3</sup> New Mexico Oil Conservation Division, OCD Geographic Information Systems <https://www.emnrd.state.nm.us/OCD/ocdgis.htm>
- <sup>4</sup> Descartes Labs, <https://www.descarteslabs.com/industries/oil-and-gas/>
- <sup>5</sup> United States Environmental Protection Agency, Greenhouse Gas Reporting Program <https://ghgdata.epa.gov/ghgp/main.do>
- <sup>6</sup> Thoma, E. S., B., OTM 33 Geospatial Measurement of Air Pollution, Remote Emissions Quantification (GMAP-REQ) and OTM33A Geospatial Measurement of Air Pollution-Remote Emissions Quantification-Direct Assessment (GMAP-REQ-DA), <https://www3.epa.gov/ttnemc01/prelim/otm33.pdf>
- <sup>7</sup> Brantley, H. L., et al., Assessment of Methane Emissions from Oil and Gas Production Pads using Mobile Measurements, *Environmental Science & Technology*, 24, 14508-14515, 2014 <https://doi.org/10.1021/es503070q>
- <sup>8</sup> Robertson, A. M., et al., Variation in Methane Emission Rates from Well Pads in Four Oil and Gas Basins with Contrasting Production Volumes and Compositions, *Environmental Science & Technology*, 15, 8832-8840, 2017, <https://doi.org/10.1021/acs.est.7b00571>
- <sup>9</sup> Caulton, D. R., et al., Quantifying uncertainties from mobile-laboratory-derived emissions of well pads using inverse Gaussian methods, *Atmos. Chem. Phys.*, 20, 15145-15168, 2018 <https://doi.org/10.5194/acp-18-15145-2018>
- <sup>10</sup> Edie, R., et al., Constraining the accuracy of flux estimates using OTM 33A, *Atmos. Meas. Tech.*, 1, 341-353, 2020, <https://doi.org/10.5194/amt-13-341-2020>
- <sup>11</sup> Edie, R., et al., Off-Site Flux Estimates of Volatile Organic Compounds from Oil and Gas Production Facilities Using Fast-Response Instrumentation, *Environmental Science & Technology*, 3, 1385-1394, 2020, <https://doi.org/10.1021/acs.est.9b05621>
- <sup>12</sup> SkyTruth, Global Flaring Dataset, <https://skytruth.org/viirs/>



- <sup>13</sup> Leak Surveys Incorporated (LSI), <https://www.leaksurveysinc.com/>
- <sup>14</sup> VIIRS Nightfire, [https://eogdata.mines.edu/download\\_viirs\\_fire.html](https://eogdata.mines.edu/download_viirs_fire.html)
- <sup>15</sup> Elvidge, C. D., et al., Methods for Global Survey of Natural Gas Flaring from Visible Infrared Imaging Radiometer Suite Data, *Energies*, 1, 14, 2016, <https://doi.org/10.3390/en9010014>
- <sup>16</sup> eCFR Title 40 Section 98.233(n)(5), <https://ecfr.io/Title-40/Section-98.233>
- <sup>17</sup> United States Environmental Protection Agency, Inventory of U.S. Greenhouse Gas Emissions and Sinks: Natural Gas and Petroleum Systems, <https://www.epa.gov/ghgemissions/natural-gas-and-petroleum-systems>
- <sup>18</sup> Barkley, Z. R., et al., Estimating Methane Emissions From Underground Coal and Natural Gas Production in Southwestern Pennsylvania, *Geophysical Research Letters*, 8, 4531-4540, 2019 <https://doi.org/10.1029/2019GL082131>
- <sup>19</sup> Barkley, Z. R., et al., Quantifying methane emissions from natural gas production in north-eastern Pennsylvania, *Atmospheric Chemistry and Physics*, 22, 13941-13966, 2017 <https://doi.org/10.5194/acp-17-13941-2017>
- <sup>20</sup> Maasakkers, J. D., et al., Gridded National Inventory of U.S. Methane Emissions, *Environmental Science & Technology*, 23, 13123-13133, 2016, <https://doi.org/10.1021/acs.est.6b02878>
- <sup>21</sup> Zhang, Y., et al., Quantifying methane emissions from the largest oil-producing basin in the United States from space, *Science Advances*, 17, eaaz5120, 2020, <https://doi.org/10.1126/sciadv.aaz5120>
- <sup>22</sup> Skamarock, W. C., et al., G.: A description of the Advanced Research WRF version 3, Citeseer, 2008 <https://doi.org/10.5065/D68S4MVH>
- <sup>23</sup> Enverus, Drillinginfo, <https://www.enverus.com>
- <sup>24</sup> United States Environmental Protection Agency, Inventory of U.S. Greenhouse Gas Emissions and Sinks: 1990-2018, <https://www.epa.gov/ghgemissions/inventory-us-greenhouse-gas-emissions-and-sinks-1990-2018>
- <sup>25</sup> Alvarez, R. A., et al., Assessment of methane emissions from the U.S. oil and gas supply chain, *Science*, 6398, 186, 2018, <http://science.sciencemag.org/content/361/6398/186.abstract>
- <sup>26</sup> Richardson, S. J., et al., Tower measurement network of in-situ CO<sub>2</sub>, CH<sub>4</sub>, and CO in support of the Indianapolis FLUX (INFLUX) Experiment, 2017, <https://doi.org/10.1525/elementa.140>
- <sup>27</sup> NOAA: Methane (CH<sub>4</sub>) WMO Scale, [https://www.esrl.noaa.gov/gmd/ccl/ch4\\_scale.html](https://www.esrl.noaa.gov/gmd/ccl/ch4_scale.html)
- <sup>28</sup> Dlugokencky, E. J., et al., Conversion of NOAA atmospheric dry air CH<sub>4</sub> mole fractions to a gravimetrically prepared standard scale, *Journal of Geophysical Research: Atmospheres*, D18, 2005 <https://doi.org/10.1029/2005JD006035>
- <sup>29</sup> Omara, M., et al., Methane Emissions from Natural Gas Production Sites in the United States: Data Synthesis and National Estimate, *Environmental Science & Technology*, 21, 12915-12925, 2018 <https://doi.org/10.1021/acs.est.8b03535>
- <sup>30</sup> PermianMAP, <https://data.permianmap.org/pages/operators>